High-Frequency Series-Resonant dc Link Power Conversion

Yoshihiro Murai, *Senior Member, IEEE*, and Thomas A. Lipo, *Fellow, IEEE*

Abstract—**A new ac/ac conversion scheme that eliminates the need for self-commutated devices and requires only 12 thyristors for full double-bridge ac-to-ac power conversion is presented. The system utilizes a series-resonant dc link between the ac/dc and dc/ac converters. This series-resonant scheme is, in effect, the dual of the parallel dc resonant converter. The dc resonant circuit can be essentially considered as a commutating circuit that ensures turnoff of all 12 thyristors by providing the necessary zero-current instants. A significantly improved sinusoidal current waveform can be obtained at both the input and output, compared with conventional high-power converters by the use of high-frequency pulse density modulation.**

INTRODUCTION

OVER THE PAST few years, remarkable progress has been made in the development of high-power density ac/ac converters using resonant-link schemes that utilize high-speed devices such as fast recovery transistors and GTO's. These new converters not only have high power density but also possess very low switching losses since switching of the devices are made at zero-voltage instants and thus enable the total system to operate at very high frequency compared with conventional dc link transistorized converters. Although these resonant-link converters are intended to operate at high power density, almost all the systems presented in the past require self-commutated transistors and have some difficulty performing conversion at very high power levels because of the relatively low voltage and current margins that self-commutated devices such as transistors typically have.

In general, switching schemes for resonant converters can be classified according to their resonant ac-link and resonant dc-link modes. Figs. 1 and 2 offer schematic illustrations of the resonant link circuits presently available [1]–[5]. The resonant ac circuits utilize a parallel resonant circuit as shown in Fig. 1(a) or a series-resonant circuit as in Fig. 1(b). The ac resonant circuit impresses both polarities of ac voltage and current on the link so that the switches of the input and output side converters are required to carry both positive and negative currents as well as block both polarities of voltage. The converter switches should therefore be bidirectional switches, which are usually realized by two inverse-parallel transistors or thyristors for the parallel and series-resonant circuits respectively, as shown in Fig. 1.

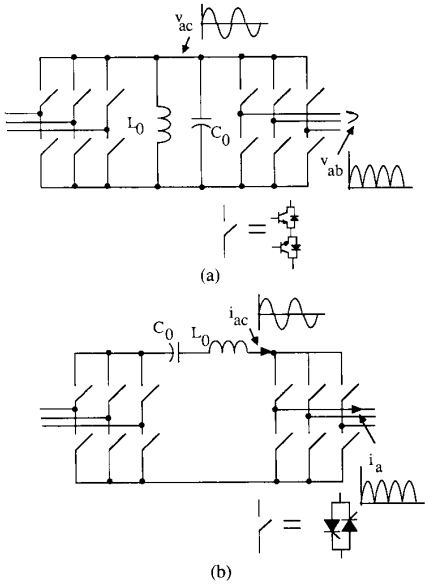

Fig. 1. Resonant ac link power converters: (a) Parallel-resonant scheme; (b) series-resonant scheme.

The dc-link circuits of Fig. 2 realize pulsating dc currents in the link by adding dc offsets to the ac resonant currents. All of the resonant dc-link converters reported in the past have been restricted to parallel resonant types [4]–[5]. As shown in Fig. 2(a), half of the transistor switches of Fig. 1(a) are replaced by diodes, and the system has a very simple configuration, much like the conventional dc link voltage source bridged converters. However, the converters still require transistors that have the self-commutating ability necessary to maintain the resonance.

The series-resonant dc-link scheme corresponding to the dual of the parallel resonant dc-link does not yet appear to have been reported in the literature. This paper develops a new series-resonant dc-link scheme utilizing a simple configuration that has only unidirectional switches as shown in Fig. 2(b). In this case, switching of the converters occurs only at the zero-crossing instants of the link current. Since the current drops below the holding current, the natural turn-off ability of a conventional SCR

Paper IPCSD 92-1, approved by the Industrial Power Conversion Committee of the IEEE Industry Applications Society for presentation at the 1988 Industry Applications Society Annual Meeting, Pittsburgh, PA, October 2–7. Manuscript released for publication February 1, 1992.

Y. Murai is with the Faculty of Engineering, Gifu University, Gifu, Japan.

T. A. Lipo is with the Department of Electrical and Computer Engineering, University of Wisconsin, Madison, WI 53706-1691.

IEEE Log Number 9203290.

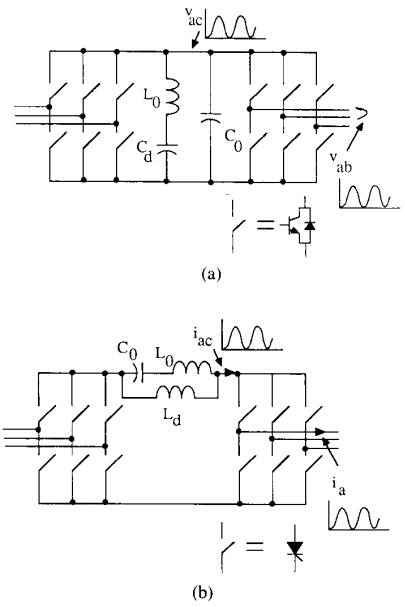

Fig. 2. Resonant dc link power converters: (a) Parallel-resonant scheme; (b) series-resonant scheme.

is utilized for commutation. Thus, high-power thyristors can thus be utilized with minimal switching loss. Since the link current is unidirectional, only the usual six thyristors are needed per converter bridge.

In this paper, the series-resonant dc-link circuit will be demonstrated to have a natural commutation capability and interruptible switching by first using a simple single-phase equivalent circuit. The three-phase configuration and various control schemes will then be reviewed. Performance of the converter will be investigated by digital simulation. It will be shown that by using pulse density modulation, this circuit will enable the realization of low distortion sinusoidal current as well as unity power factor on both the ac/dc and dc/ac side converters.

Finally, the paper discusses the possible oscillations in the output, which seems to be a common problem with pulse-modulated current source systems. The use of derivative feedback and damping circuits are discussed for the purpose of stabilization.

Principle of Operation of Proposed Circuit

A more complete depiction of the series-resonant dc-link converter is shown in Fig. 3. The inductor L_0 and capacitance C_0 are the resonant elements selected to resonate at a frequency consistent with the turn-off capability of the converter, which is typically 10–20 kHz, and are relatively small. The thyristor T_{crc} is a protection device, is not normally active, and is used to circulate the current in the resonant circuit and ensure turnoff when the link is not requested to supply current to the load. The inductor L_d is a larger inductor that is controlled to support the dc bias current.

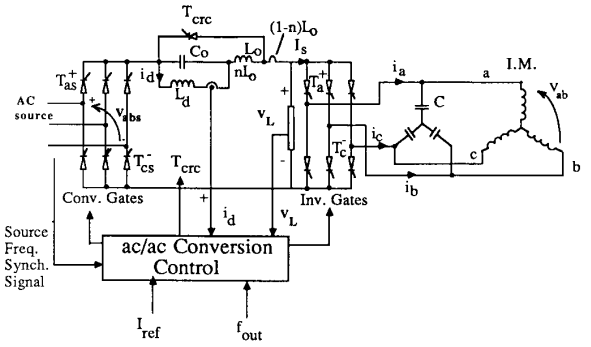

Fig. 3. Detailed circuit proposed for implementing the series-resonant dc link scheme.

Fig. 4 shows the principle of operation of the basic series-resonant dc-link circuit. The currents in Fig. 4(a) are obtained from the following equations:

$$E = \frac{1}{C_0}\int_0^t i_0\,dt + L_0\frac{di_0}{dt} + V_L \tag{1}$$

$$E = L_d\frac{di_d}{dt} + V_L \tag{2}$$

$$V_L = \frac{1}{C}\int_0^t i_s\,dt \tag{3}$$

$$i_s = i_0 + i_d. \tag{4}$$

Assume the thyristor T_h shown in Fig. 4 is switched to the conducting state at $t = 0$. If L_d and C_L are sufficiently large to maintain the current i_d and voltage V_L constant, then the current i_s is easily solved by defining the initial conditions

$$i_d = I_d, \qquad i_0 = -I_d$$
$$(i_s = 0, \qquad \text{at } t = 0)$$
$$v_c = V_{c0} \tag{5}$$

where I_d and V_{c0} are constants. The solution to these differential equations is

$$i_0 = \sqrt{\frac{C_0}{L_0}}\,E' \sin \omega t - I_d \cos \omega t \tag{6}$$

$$\omega = \sqrt{\frac{1}{L_0C_0}}$$

and

$$i_s = i_0 + i_d$$
$$= \sqrt{\frac{C_0}{L_0}}\,E' \sin \omega t + I_d(1 - \cos \omega t) \tag{7}$$

where $E' = E - v_L + v_{C0}$ (> 0).

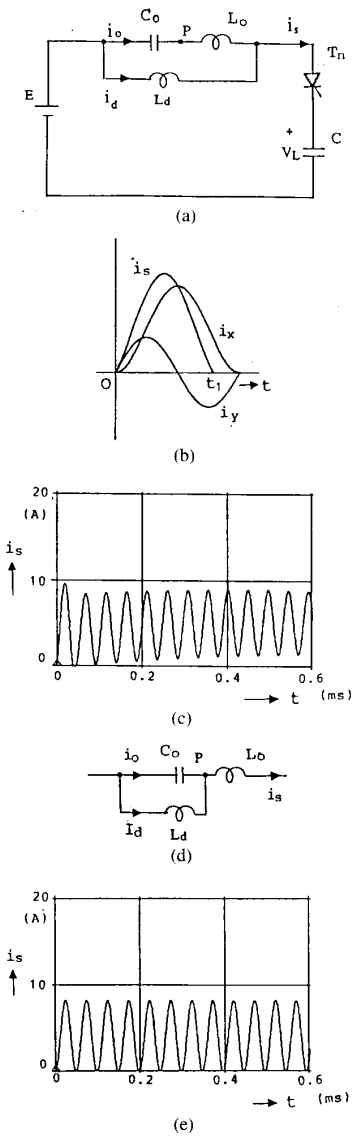

Fig. 4. Principle of operation of the series-resonant circuit: (a) series-resonant circuit with parallel inductance L_d; (b) currents corresponding to the circuit of (a); (c) actual current i_s for the circuit of (a); (d) modification of the connection point of L_d; (e) actual current i_s for circuit of (d).

Letting

$$i_x = I_d(1 - \cos \omega t), \qquad i_y = \sqrt{\frac{C_0}{L_0}}\, E' \sin \omega t \quad (8)$$

the current in the link can then be written as

$$i_s = i_x + i_y.$$

Typical waveforms for the currents i_x, i_y, and i_s are shown in Fig. 4(b). As long as the voltage E' remains positive, the link current reaches zero, and thyristor T_h is able to commutate at $t = t_1$. Unfortunately, however, in actual circuit with finite L_d and C_L, the current i_d continues to increase if E' is positive, and this fact makes the commutation of thyristor T_h very difficult, as shown in Fig. 4(c).

Fig. 4(d) shows an improved connection in which L_d is connected in parallel with capacitance C_0. As the voltage across L_d changes according to the capacitor voltage V_0, commutation of the thyristor becomes possible because the resonant current has an oscillation that is not growing, as shown in Fig. 4(e).

In order to prevent overcharging of the resonant capacitor during the zero current intervals, a circulating thyristor T_{crc} has been utilized as shown in Fig. 5. This thyristor is triggered to circulate the current i_0 whenever i_s becomes zero. (This zero current condition is also required to regulate the output current of the inverter for pulse density modulation and will be described later).

Figs. 5(b) and (c) show the current i_s and V_L both with and without use of the circulating current thyristor T_{crc}. When a signal to stop firing T_h occurs, a dead zone appears as shown in Fig. 5(b). As a result, the average output voltage does not change, and a large pulse of current appears when conduction of T_h commences. Alternatively, for the case with thyristor T_{crc}, the current i_s is readily interrupted while a triggering signal is set to zero, and a current i_{crc} flows during this period as shown in Fig. 5(c).

In practice, the circulating thyristor is fired not only when the stop signal for i_s appears but also functions as a clipper for i_s and V_L, in which case, the resonance of the L-C tank becomes quite stable. The tap ratio n ($n < 1$) of the inductance L_0 affects the sensitivity of the clipping ability of T_{crc}. If n is set to a large value, the overshoot of current i_s and the voltage V_L increase, and the resonance tends to become unstable. On the other hand, when n is chosen very small (nearly 0), the current i_s goes to zero rapidly whenever the voltage V_l becomes equal to E, and the necessary zero current condition cannot be attained. In this paper, a tap ratio of $n = 0.1$ is utilized.

In order to maintain control of the amplitude of the pulses as illustrated in Fig. 4(e), regulation of the dc link current is required. Figs. 6(a) and (b) illustrate how the link current varies with and without regulation. In general, the average value of the current pulse is approximately proportional to i_d. When E' is large, i_s increases and i_d also increases, as shown in Fig. 6(b). After i_s reaches zero at $t = t_1$, T_h turns off, and current i_d charges up C_o generally to a larger value than that which existed on the capacitor before the previous pulse. After each subsequent turnon of the thyristor T_h, the currents i_d and pulses i_s continue to increase as shown. Hence, current regulation for this type of converter is a mandatory condition.

Regulation of the dc inductor current i_d is accomplished very easily by current feedback as shown in Fig. 6(c). After comparing i_d with the current reference I_{dref}, the source voltage E is adjusted to make the error small.

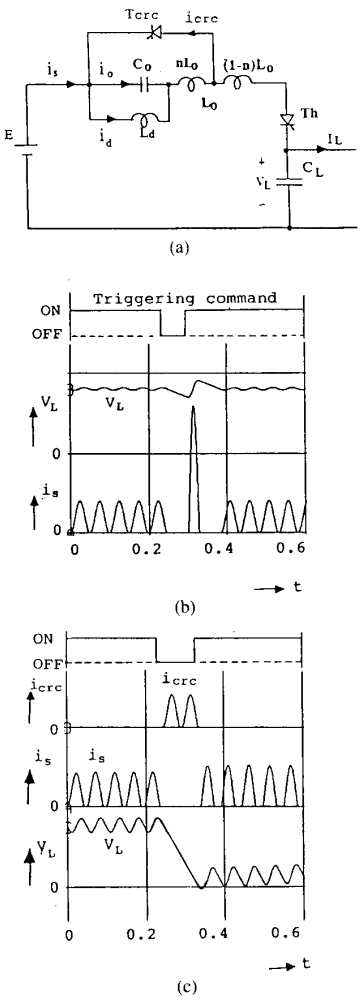

Fig. 5. Illustrating purpose of circulating current thyristor: (a) Series-resonant circuit with circulating current thyristor; (b) circuit behavior without T_{crc}; (c) circuit behavior with T_{crc}.

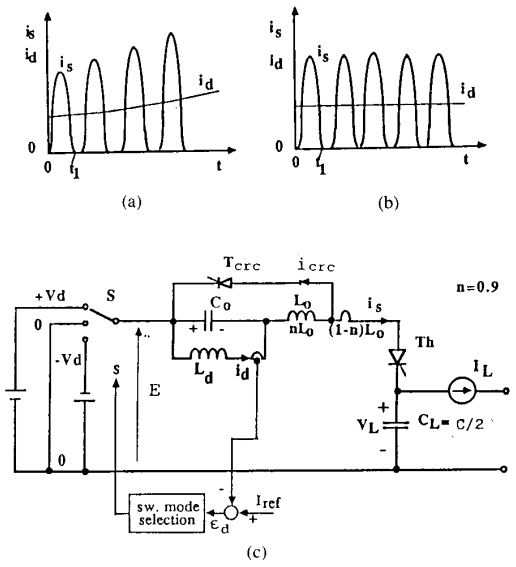

Fig. 6. Current control of dc inductance: (a) noncontroled i_d; (b) controled i_d; (c) current control scheme.

For example, the error $\epsilon_d = I_{dref} - I_d$ is positive, and E is changed from V_d to 0 or $-V_d$; if ϵ_d is negative, it goes vice versa. As the controlling ability to i_d also depends on E' $(= E - V_L)$, the measured value of V_L is used for this purpose. Although the thyristor T_h is off, L_d charges up C_0 to a negative polarity to prepare for conduction of T_h. The current i_s carries the energy from the resonant circuit to the load or ac source, depending on the polarity of V_L and E. When E is negative, energy flows back to source, and when V_L is positive, the energy also flows to load.

Thus far, it has been assumed that the source voltages are essentially constant. Since the source voltages are, in fact, alternating, the identity of the most positive and most negative phase must be established before switching of the source side bridge can commence. The selection of the source voltages are easily accomplished as shown in Fig. 7. When positive, a large positive voltage E' is needed to cause the current i_d to increase. The thyristors are triggered as shown in heavy lines in Fig. 7(a) and supply positive voltage V_d to the resonant current. Fig. 7(b) shows the zero voltage mode and Fig. 7(c) the negative voltage mode. These modes are used to decrease the current i_d. As i_s is always positive, mode (c) regenerates energy back to the ac source.

Three-Phase Configuration

In the three-phase configuration, the pulses generated in the resonant circuit must be distributed to each phase. The thyristors in Fig. 3 function as a distributor to switch or redirect the link current at the instants where the current $i_s = 0$. Since the circuit is resonant, this instant occurs when nearly zero voltage exists across the thyristor so that the losses in the thyristors are relatively small. Fig. 8 shows an example of the pulse density distribution for each phase in the output of the dc/ac side converter.

The distribution of the pulses to each phase is illustrated in Fig. 8 and are automatically determined by comparing the current pulses with the instantaneous phase currents. Fig. 9 shows the current references i_{1r} and i_{2r}, the corresponding phase currents i_{sa}, i_{sb}, and i_{sc}, and the conducting thyristors in the converter. For example, the current references i_{1r} and i_{2r} correspond to i_{sa} and i_{sb} within the first 60° at which point thyristors T_a, T_b, T_c are triggered. In the next 60°, these currents correspond to $-i_{sc}$ and $-i_{sa}$, thyristors T_c, T_a, T_b are triggered, and so on. Accordingly, the same reference table is repetitively used and makes the ROM table very small. The currents i_1 and i_2 are detected from a current sensor with sampling switch S as shown in Fig. 9(b), which is operated synchronized to the triggering signal of the dc/ac converter thyristor firing instants.

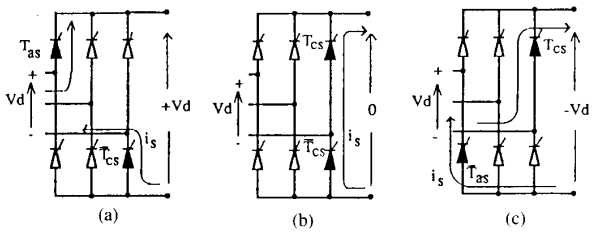

Fig. 7. Illustrating ac/dc conversion modes: (a) Motoring mode; (b) circulating mode; (c) regenerating mode.

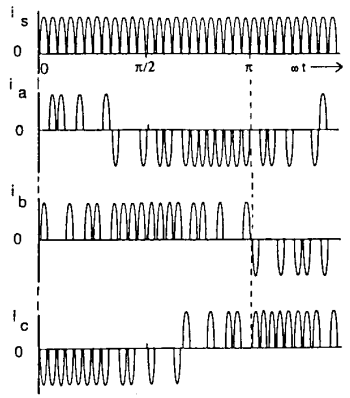

Fig. 8. Illustrating distribution of current pulses to a three-phase load.

Triggering Scheme

The dc/ac converter thyristors are triggered to reduce the maximum error of the three-phase currents. Errors $\epsilon_a, \epsilon_b, \epsilon_c$ are obtained from ϵ_1, ϵ_2, as defined by the chart in Fig. 9(c). Fig. 10 shows the possible combinations of the errors $\epsilon_a, \epsilon_b, \epsilon_c$ for i_{sa}, i_{sb}, i_{sc}, respectively.

As the sum of the errors must satisfy the relation

$$\epsilon_a + \epsilon_b + \epsilon_c = 0. \tag{9}$$

All three errors clearly cannot have the same polarity. Because the output circuit does not have any neutral line, the current pulse should flow into the positive error phase and flow out from the negative error phase. Hence, the triggering principle is as follows:

1) The thyristor in the phase having the larger error out of the two phases of the same polarity is chosen to be triggered.
2) The phase corresponding to the error with the opposite polarity error is selected as the other triggering phase.

For example, in Fig. 10, if ϵ_a and ϵ_b are positive, then ϵ_c must be negative. This condition can be termed as mode 1. If ϵ_a is larger than ϵ_b, the triggering thyristor is selected to be T_a, and the other thyristor becomes T_c. Fig. 11 shows the schematic diagram of the overall control system. The mode matrix and comparison gate of currents are included in the block "switching matrix." The ac/dc

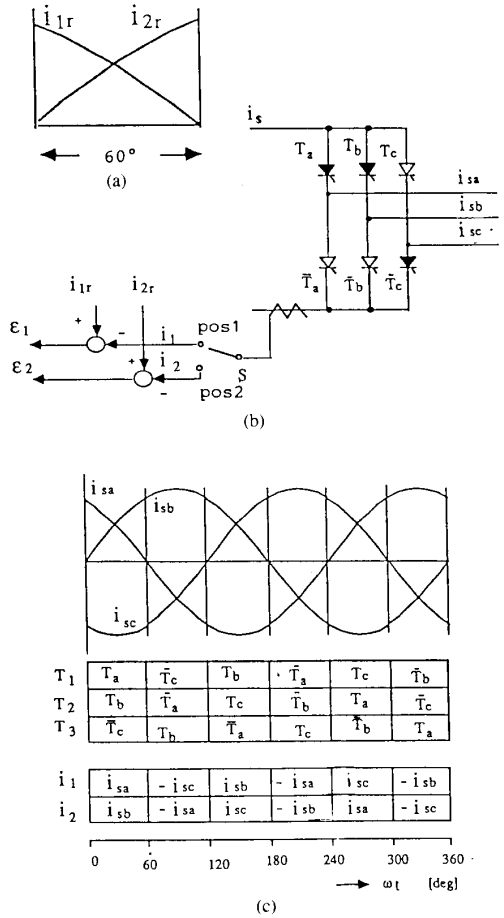

Fig. 9. Current references and the corresponding current and thyristor selection for each 60° interval: (a) Current references; (b) current feedback selection circuit; (c) current and thyristor selection table.

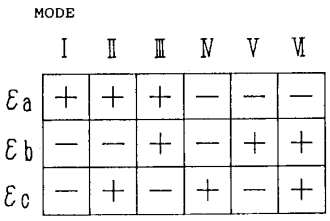

Fig. 10. Polarity of current error for each of the operating modes.

thyristors are triggered by applying the chart shown in Fig. 9(c). The thyristors shown on the chart are triggered when positive V_d is required on the dc side, and these patterns are synchronized to the ac input voltage by the timing pulse f_{in}.

When a negative voltage $E = -V_d$ is required, the triggering thyristors in the chart are replaced from the top to the bottom or from the bottom to the top of the bridge. As explained previously, thyristor T_{crc} is not triggered,

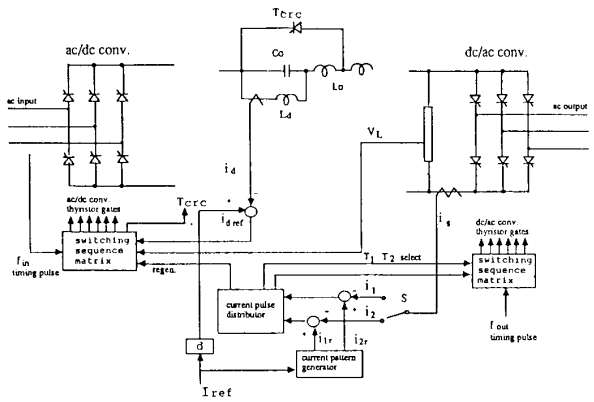

Fig. 11. Control diagram for the overall system.

when $E' = E - V_L$ is less than V_d (> 0). Current i_d is regulated to a value three times that of I_{dref} ($k_d = 3$) in order to ensure sufficient gain to control the load current.

Resulting Waveforms

Fig. 12 shows the resulting current waveforms obtained by computer simulation. A three-phase $R - L$ load with back emf has been utilized. Fig. 12(a) was obtained for the case $R = 5\ \Omega$, $L = 1.0$ mH, $E = 100$ V, $\phi = -10°$, $L_d = 5$ mH, $L_0 = 79\ \mu$H, $C_0 = 0.79\ \mu$F, and $\omega_0 = 2\pi \times 20\,000$ rad/s. In addition, the actual simulation includes a resistance $r_o = 0.05\ \Omega$ as part of the inductor L_0 to express the lossy component in the resonant circuit. The waveform appears to be very satisfactory. However, when the resistance R and inductance L are replaced by an induction motor load (200 V, 1.5 kw), i.e., $R = 1.0\ \Omega$ and $L = 2$ mH, a high-frequency oscillation appears as shown in Fig. 14(b). This oscillation is clearly caused by interaction of the filter capacitance C and motor load inductance L. Since the loop of the oscillation involves two C's and two L's in series, the resonant frequency f_r is

$$f_r = \frac{1}{2\pi\sqrt{(2L)(C/2)}} = \frac{1}{2\pi\sqrt{LC}}. \qquad (10)$$

For this case, $f_r = 1250$ Hz. This phenomena appears to be a generic problem for any current-source inverter having output capacitance and is not peculiar to this circuit alone.

Stabilization

The stabilization of the system is difficult by controlling the current i_s only. Even if the system is accurately controlled, the oscillation remains between the capacitor C and load inductance L almost independent of the current from the inverter i_s. Stabilization was, however, accomplished by controlling the motor currents i_a, i_b, i_c instead of the output currents i_{sa}, i_{sb}, i_{sc}. Fig. 13 shows the current feedback loop with a derivative element. Two loops are needed to obtain i_a, i_b, and i_c. In this case, ac link frequency corresponding to L_0 and C_0 is almost

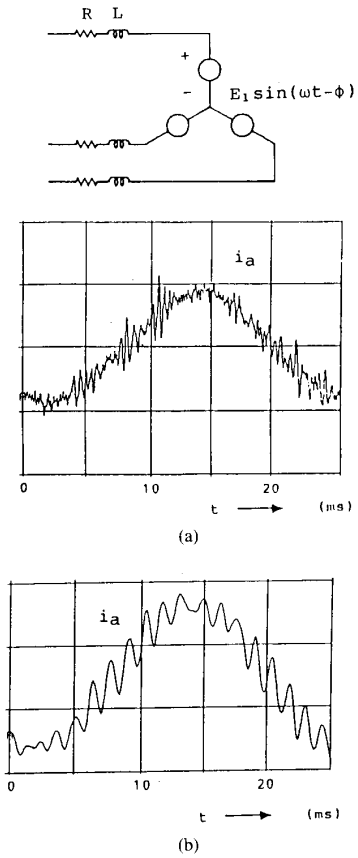

Fig. 12. Output line currents obtained by digital simulation: (a) Circuit load model and current waveform for the case $R = 5.0\ \Omega$, $E_1 = 100$ V, $\phi = 100°$; (b) current waveform utilizing an induction motor model, $R_1 = 1.0\ \Omega$, $L_1 + L_2 = 4.0$ mH.

completely filtered by the load capacitances C. Hence, feedback was easily done without any further filtering. The derivative circuit was implemented by a simple $R - C$ circuit, as shown in Fig. 13(a). The time constant was selected as 50 μs, and the gain was 2.0. The resulting waveform is shown in Fig. 13(c) and can be compared with the case without derivative feedback, i.e., $K_{drv} = 0$ in Fig. 13(b). The system is completely unstable as shown in Fig. 13(b), but the system is stabilized by using derivative feedback, although it still has an oscillation as shown in Fig. 13(c). The remaining high-frequency oscillation over 2 kHz does not have the frequency of (10) and seems not to be caused by system instability but is ripple caused by the discrete current pulses.

Damping Circuit

In order to further reduce or absorb the high-frequency component caused by the current pulses, the damper circuit shown in Fig. 14(a) has been found to be effective. The damping circuit utilizes a resistance R_{dmp} and capacitance C_{dmp}. If the voltage of the ripple component is assumed to be E_{rpl} in the expression of the rms phasor,

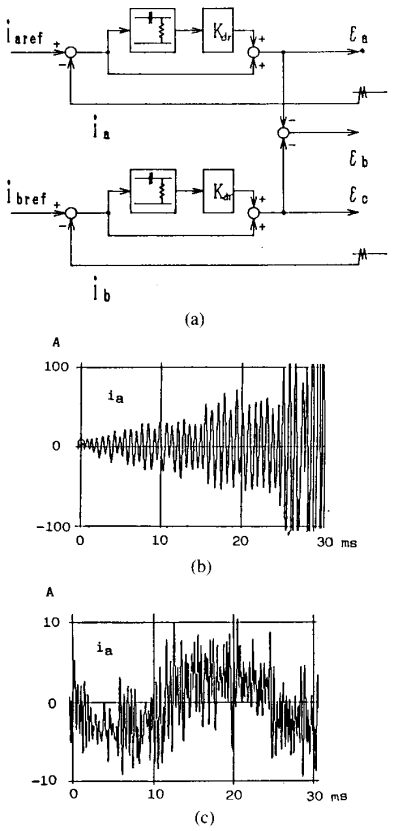

Fig. 13. Simulated results employing output current feedback: (a) Current feedback loop; (b) without derivative feedback; (c) with derivative feedback.

the current through R_{dmp} is obtained from

$$I_{dmp} = \frac{E_{rpl}}{\sqrt{R_{dmp}^2 + \dfrac{1}{\omega_{rpl}^2 C_{dmp}^2}}} \tag{10}$$

and the dissipated energy P_{dss}in R_{dmp} will be

$$P_{dss} = I_{dmp}^2 R_{dmp} \quad \text{(for the single phase model)}$$

$$= E_{rpl}^2 C_{dmp} \Bigg/ \left[\left(\sqrt{R_{dmp}} - \frac{1}{\sqrt{R_{dmp}} C_{dmp} \omega_{rpl}} \right)^2 + \frac{2}{\omega_{rpl} C_{dmp}} \right]. \tag{11}$$

Hence, the resistance R_{dmp} is selected as

$$R_{dmp} = \frac{1}{\omega_{rpl} C_{dmp}} \tag{12}$$

and the maximum dissipation P_{dmax} can be calculated in

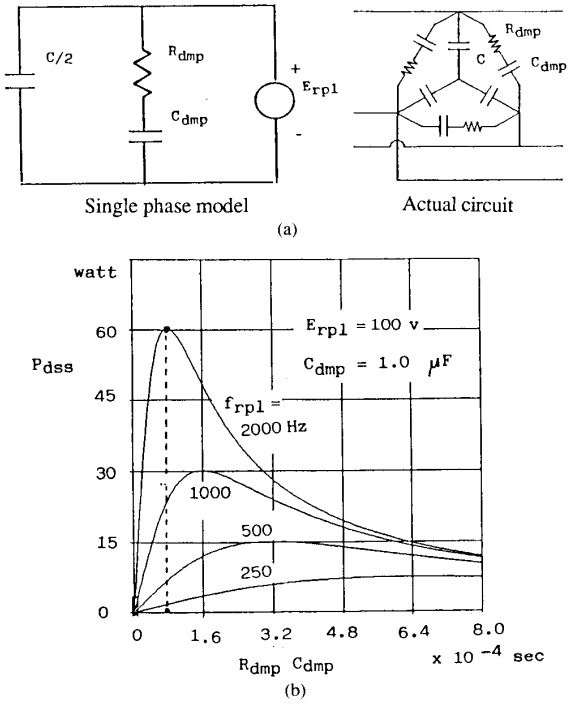

Fig. 14. Damping circuit for attenuating load current oscillation: (a) R–C damping circuit; (b) dissipated energy in damping resistor R_{dmp}.

the form

$$P_{dmax} = E_{dmp}^2 C_{dmp} \omega_{rpl}. \tag{13}$$

When (12) is satisfied, the dissipation in the output at fundamental frequency becomes extremely small. Fig. 14(b) shows the dissipation P_{dss} as a function of the time constant $\tau_{dmp} = R_{dmp} C_{dmp}$ and ripple frequency f_{rpl} when the capacitance C_{dmp} is assumed constant, for example, if the ripple frequency and capacitance C_{dmp} are assumed to be 2000 Hz and 1.0 μF, respectively. Then, R_{dmp} becomes 80 Ω from (9), and the time constant $\tau_{dmp} = R_{dmp} C_{dmp} = 80$ μs.

If the fundamental frequency is 50 Hz, then from the characteristic for $\tau_{dmp} = 80$ μs in Fig. 14(b), the dissipated energy both in ripple frequency and in fundamental frequency are

$$\begin{aligned} P_{dss} &= 60 \text{ W (2000 Hz)} \\ &= 0.56 \text{ W (50 Hz)}. \end{aligned} \tag{14}$$

Hence, the fundamental component is negligible, dominant dissipating energy is the ripple component, and very strong selective frequency damping will be performed.

Fig. 15(a) and (b) are the results of using damping circuit for the cases in Fig. 13(b) and (c), respectively. Substantial improvement is apparent in both cases. In the case of nonderivative feedback (Fig. 15(b)), the system was stabilized, and a much smaller ripple in the current was obtained. As shown in the figure, the damping capacitance is almost comparable with the output capacitance; therefore, the capacitance C's are increased in Fig. 16(c),

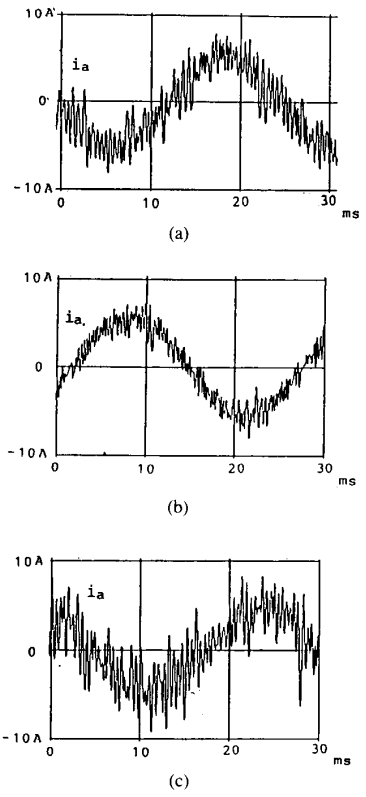

Fig. 15. Output current waveforms illustrating the effects of damping circuit: (a) With damping circuit only; (b) with both derivative feedback and damping circuit; (c) with neither damping circuit nor derive feedback.

whereas the other parameters are the same as in Fig. 15(b). Although a better result was obtained in Fig. 15(c), this waveform still contains a larger ripple than in Fig. 15(b). Accordingly, it can be said that damping capacitance is much more effective in reducing the high-frequency current ripple than in increasing the output capacitance value. However, the high-frequency loss in the damper may increase for machines with very low losses, and an upper limit exists from the point of view of total efficiency.

It should be mentioned, finally, that more recent work on this topic has lead to the use of an inner voltage loop for stabilization. This research has been the topic of a companion paper [6].

Conclusion

In this paper, a new high-frequency series-resonant dc-link ac/ac conversion scheme was described. This new resonant scheme was accomplished by introducing a dc inductance in parallel with a series-resonant circuit, thus enabling the system to operate with only unidirectional current conducting, bidirectional voltage blocking switches, i.e., thyristors. In addition, the number of the switching devices has been reduced to half the number required in the conventional ac resonant current link. Accordingly, very high levels of power conversion can be realized since the thyristor retains very high margins of voltage and current compared with the transistors utilized in conventional high-frequency resonant ac/dc voltage link converters. As this scheme utilizes current pulse density modulation, the output current waveform is significantly improved. Since the input side ac/dc converter also utilizes the same modulation algorithm, the input current waveform becomes sinusoidal, and operation at unity power factor is available.

In this paper, a circuit with a circulating thyristor was proposed to ensure natural commutation of the converter thyristors. The thyristor serves to circulate a current equal to three times of the load current so that very high response will be obtained, even if the loading condition is suddenly changed.

Finally, the paper has also been concerned with the oscillations and instability arising from the output capacitance and inductive load when supplied from a current source inverter. Derivative feedback and damping circuits were utilized and were shown to be an effective means for reducing these undesirable components.

References

[1] P. Sood and T. A. Lipo, "Power conversion distribution system using a resonant high-frequency ac link," in *IEEE-IAS Ann. Mtg. Conf. Rec.*, 1986, pp. 533–541.

[2] H. K. Lauw, J. B. Klaassens, N. G. Butler, and D. B. Seely, "Variable-speed generation with the series-resonant converter," in *IEEE-PES Winter Mtg. Conf. Rec.*, 1987/1988.

[3] S. W. H. de Haan and J. D. Lodder, "A formalistic approach to series-resonant power conversion," in *EPE Conf. Rec.*, 1987, pp. 231–238.

[4] D. M. Divan, "The resonant dc link converter—A new concept in static power conversion," in *IEEE IAS Ann. Mtg. Conf. Rec.*, 1986, pp. 648–656.

[5] D. M. Divan and G. L. Skibinski, "Zero switching loss inverters for high-power applications," *IEEE IAS Ann. Mtg. Conf. Rec.*, 1987, pp. 627–634.

[6] P. Caldeira, T. A. Lipo, Y. Murai, and S. Mochizuki, "Design and control of a series resonant dc link power converter drive," in *Proc. 1990 Int. Power Electron. Conf.* (IPEC) (Tokyo, Japan), Apr. 1990, pp. 397–404.

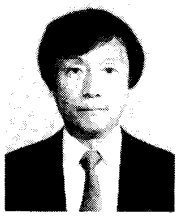

Yoshihiro Murai (A'85–SM'91) was born in Sagamihara-city, Japan, on January 13, 1942. He received the B.S. and M.S. degrees in 1965 and 1969, respectively, from Gifu University. He received the Dr.Eng. degree from Tokyo Institute of Technology in 1981.

Since 1969, he has been engaged in the field of power electronics, especially in inverter-driven motor systems, brushless dc motors, high-frequency resonant link converters, PWM technique, and stability analysis. He is currently a professor at Gifu University. He stayed for ten months at the University of Wisconsin-Madison from 1987 to 1988, where he began work on the series-resonant dc link converter.

Dr. Murai is a member of SICEJ and IPE of Japan.

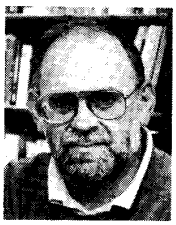

Thomas A. Lipo (M'64–SM'71–F'87) is a native of Milwaukee, WI. He received the B.E.E. and M.S.E.E. degrees from Marquette University, Milwaukee, WI, in 1962 and 1964 and the Ph.D. degree in electrical engineering from the University of Wisconsin in 1968.

From 1969 to 1979, he was an electrical engineer in the Power Electronics Laboratory of Corporate Research and Development of the General Electric Company, Schenectady, NY. He became Professor of Electrical Engineering at Purdue University in 1979, and in 1981, he joined the University of Wisconsin in the same capacity, where he is presently the W. W. Grainger Professor of Power Electronics and Electrical Machines.

Dr. Lipo has maintained a deep research interest in power electronics and ac drives for over 25 years. He has received 11 patents and has 13 IEEE prize paper awards for his work, including corecipient of the Best Paper Award in the IEEE TRANSACTIONS ON INDUSTRY APPLICATIONS for the year 1984. In 1986, he received the Outstanding Achievement Award from the IEEE Industry Applications Society for his contributions to the field of ac drives, and in 1990, he received the William E. Newell Award of the IEEE Power Electronics Society for contributions to the field of power electronics.